An electron paramagnetic resonance study of electron–hole asymmetry in charge ordered $Pr_{1-x}Ca_xMnO_3$ (x = 0.64, 0.36)

2004 J. Phys.: Condens. Matter 16 2869

(http://iopscience.iop.org/0953-8984/16/16/011)

INSTITUTE OF PHYSICS PUBLISHING JOURNAL OF PHYSICS: CONDENSED MATTER

J. Phys.: Condens. Matter **16** (2004) 2869–2878 PII: S0953-8984(04)73109-4

An electron paramagnetic resonance study of electron–hole asymmetry in charge ordered $Pr_{1-x}Ca_xMnO_3$ (x = 0.64, 0.36)

Janhavi P Joshi[1], **K Vijaya Sarathy**[2], **A K Sood**[1], **S V Bhat**[1,3] **and C N R Rao**[2]

[1] Department of Physics, Indian Institute of Science, Bangalore 560 012, India
[2] Chemistry and Physics of Materials Unit, Jawaharlal Nehru Centre for Advanced Scientific Research, Jakkur PO, Bangalore 560 064, India

E-mail: svbhat@physics.iisc.ernet.in

Received 6 December 2003
Published 8 April 2004
Online at stacks.iop.org/JPhysCM/16/2869
DOI: 10.1088/0953-8984/16/16/011

Abstract

We present and compare the results of temperature-dependent electron paramagnetic resonance (EPR) studies on $Pr_{1-x}Ca_xMnO_3$ for $x = 0.64$, which is electron-doped, with results of studies on the hole-doped, $x = 0.36$ composition. The temperature dependence of the various parameters obtained from the powder and single crystal spectra show significant differences between the two manganites. At room temperature the 'g' parameter for the electron-doped system is less than the free electron 'g' value 'g_e', whereas for the hole-doped system it is more than 'g_e'. Further, the linewidth obtained from the powder spectra as well as the single crystal spectra show different functional dependences on temperature in the two systems. Quite strikingly, the peak observed at T_{co} in the temperature dependence of the asymmetry parameter, α, of the single crystal spectra in the hole-doped system, is absent in the electron-doped system. We understand this contrasting behaviour of the EPR parameters in the two systems in terms of the very different nature of microscopic interactions in them.

1. Introduction

The phenomenon of charge ordering observed in $Re_{1-x}A_xMnO_3$, where Re is a trivalent rare earth ion and A is a divalent alkaline earth ion, has been intensively studied over the past few years. This phenomenon has been one of the most puzzling of the various properties exhibited by the rare earth manganites, such as colossal magnetoresistance (CMR), orbital ordering,

[3] Address for correspondence: Department of Physics, Indian Institute of Science, Bangalore-560012, India.

phase separation and a large number of magnetic and structural transitions as a function of temperature and composition [1, 2]. The parent compound $ReMnO_3$ contains Mn^{3+} ions which have one outermost e_g electron. Doping with a divalent alkaline earth ion introduces Mn^{4+} with one less electron (a hole) and hence manganites with $x < 0.5$ are called 'hole-doped'. Coming from the opposite end of the phase diagram the $AMnO_3$ compound consists of all Mn^{4+} ions and doping it with a trivalent rare earth ion introduces Mn^{3+} ions and hence e_g electrons into the system. Therefore, manganites with $x > 0.5$ are termed 'electron-doped'. Interestingly, the phase diagram is not symmetric across $x = 0.5$ concentration, though the number of charge carriers on both sides of $x = 0.5$ varies in a symmetric manner. Broadly speaking, the $x < 0.5$ region in the phase diagrams of the manganites is dominated by ferromagnetic interaction, whereas the $x > 0.5$ region is characterized by charge ordering. The phase diagram of $Pr_{1-x}Ca_xMnO_3$ (PCMO) shows charge ordering in the $0.3 < x < 0.8$ composition regime. However, the asymmetry of the phase diagram persists even in the charge ordered (CO) state of $x < 0.5$, e.g. $x = 0.36$ (PCMO-h), and $x > 0.5$ compound, e.g. $x = 0.64$ (PCMO-e). The properties of the CO state are quite different in the two compounds. The charge ordering transition temperature T_{co} for PCMO-h is 240 K whereas that for PCMO-e is 268 K. Charge ordering in the former can be melted into a ferromagnetic metallic state by doping with ions such as Cr^{3+} and Ru^{4+} and also by the application of magnetic fields, whereas no such signs of melting of charge order are observed in PCMO-e. The nature and the origin of these differences have been the subject of recent studies and this 'electron hole asymmetry' has been attributed to the intrinsic differences in the electronic structure of the two types of systems [3].

Electron paramagnetic resonance (EPR) has proved to be a valuable tool in the study of the manganites. Through a study of the temperature and composition dependence of various EPR parameters, such as the linewidth and the intensity across the various transitions, valuable information has been obtained regarding the interplay of different interactions in the systems [4–11]. However, most of these studies relate to CMR manganites and there are comparatively very few published reports of EPR studies of CO manganites [12, 13, 15]. In the CMR manganites the studies so far have mostly focused on the paramagnetic regime ($T > T_c$) because in the ferromagnetically ordered phase many extrinsic factors such as demagnetizing fields, size and shape effects and magnetic inhomogeneities affect the EPR signals. Since the charge ordered state is not magnetically ordered, EPR in CO manganites is expected to be free of such problems. However, it is to be kept in mind that magnetic correlations can still be present in a way similar to their presence in the paramagnetic phase of CMR manganites. In fact the neutron scattering work of Kajimoto *et al* on $Pr_{1-x}Ca_xMnO_3$ and Bao *et al* on $Bi_{1-x}Ca_xMnO_3$ show that when these materials are cooled below T_{co}, ferromagnetic correlations weaken and antiferromagnetic correlations grow stronger as the T_N is approached. Conceivably these correlations can have some effect, such as net local fields in single crystal samples, on the EPR parameters if their timescales happen to be comparable to the inverse of the interaction strength. Thus the EPR in charge ordered manganites is expected to be interesting as well as different from that in CMR manganites. This expectation was borne out by our earlier studies on hole-doped $Pr_{1-x}Ca_xMnO_3$ [12] and $Nd_{0.5}Ca_{0.5}MnO_3$ [13].

To the best of our knowledge, there has been no report of a comparative EPR study of electron- and hole-doped manganites, particularly in their charge ordered state. Since the asymmetry in the phase diagram across $x = 0.5$ is an interesting aspect of the physics of manganites, we compare the EPR results on the electron-doped manganite $Pr_{0.36}Ca_{0.64}MnO_3$ (PCMO-e) with those reported by us earlier [12] on the hole-doped $Pr_{0.64}Ca_{0.36}MnO_3$ (PCMO-h) with a view to understanding this asymmetry as reflected in the EPR parameters and their temperature dependence.

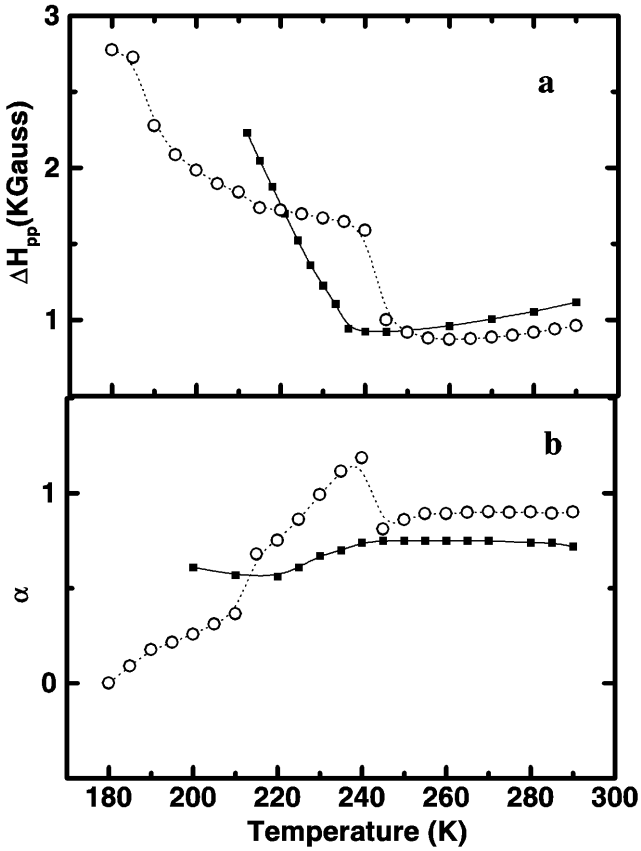

Figure 1. Temperature dependence of single crystal lineshape parameters: (a) peak to peak linewidths ΔH_{pp} and (b) the asymmetry parameter α; the error bars for ΔH_{pp} and α are very small and hence are not shown. The open circles represent the data for PCMO-h and the solid squares for PCMO-e. The curves (dotted and solid, respectively) are guides to the eye. The data for PCMO-h are reproduced for the sake of comparison from [12].

2. Experimental details

Single crystals of PCMO-e were prepared by the float zone technique. Resistivity measurements show an increase in the resistivity at $T_{co} = 268$ K. Magnetization measurements show a peak in the susceptibility also at 268 K. However no peak in the susceptibility was observed at T_N unlike in PCMO-h.

The EPR experiments were carried out on both single crystal and powder samples of PCMO-e using a Bruker X-band spectrometer (model 200D) equipped with an Oxford Instruments continuous flow cryostat (model ESR 900). The spectrometer was modified by connecting the X and Y inputs of the chart recorder to a 12 bit A/D converter which in turn is connected to a PC enabling digital data acquisition. With this accessory, for the scanwidth typically used for our experiments, i.e. 6000 G, one could determine the magnetic field to a precision of ± 3 G. For single crystal study the static magnetic field was kept parallel to the c-axis of the crystal. Experiments were also performed with another orientation ($H \parallel a$) to check for any anisotropy in the ESR response. For powder measurements, the single crystal was finely ground and dispersed in paraffin wax. The temperature was varied from 4.2 K to room

temperature (accuracy: ± 1 K) and the EPR spectra were recorded while warming the sample. Signals could be recorded only for temperatures $T > 200$ K below which signals had very poor signal to noise ratio. While doing experiments on both the single crystal and the powder, a speck of DPPH was used as a g-marker. To carry out the lineshape fitting (to be described below) the signal due to DPPH was subtracted digitally.

3. Results and discussion

The EPR signals obtained from the single crystal samples of PCMO-e are Dysonian in shape, just as in the case of PCMO-h [12]. The signals are fitted to the equation [10]

$$\frac{\mathrm{d}P}{\mathrm{d}H} = \frac{\mathrm{d}}{\mathrm{d}H} A\left(\frac{\Delta H + \alpha(H - H_0)}{4(H - H_0)^2 + \Delta H^2} + \frac{\Delta H + \alpha(H + H_0)}{4(H + H_0)^2 + \Delta H^2}\right) \tag{1}$$

where ΔH is the full width at half intensity, A is the area under the absorption curve, H_0 is the resonance field and α is the asymmetry parameter which is the fraction of the dispersion component of the Lorentzian lineshape function added to the absorption component resulting in the Dysonian lineshape. As is well known, such lineshapes are observed when the sample dimensions are larger than the skin depth. In equation (1) the first term represents the signal response due to the component of microwaves that is polarized clockwise and the second term represents the response to the component polarized anticlockwise. The large linewidth makes the inclusion of both the components necessary [10]. The peak to peak linewidth ΔH_{pp} ($=\Delta H/\sqrt{3}$) and the asymmetry parameter α obtained from the fits to the equation (1) are plotted in figure 1 against temperature. The single crystal data of PCMO-h obtained by us earlier [12] are also plotted in the same figure for the purpose of comparison.

The EPR spectra from the powder sample of PCMO-e are Lorentzian in shape, again similar to those from powder samples of PCMO-h, and are fitted to the equation

$$\frac{\mathrm{d}P}{\mathrm{d}H} = \frac{\mathrm{d}}{\mathrm{d}H} A\left(\frac{\Delta H}{4(H - H_0)^2 + \Delta H^2} + \frac{\Delta H}{4(H + H_0)^2 + \Delta H^2}\right) \tag{2}$$

where the symbols have the same meanings as in equation (1). The two terms are also incorporated for the same reason as mentioned above. From the best fit value of the resonance field H_0 the effective 'g' parameter is obtained from the resonance condition: $h\nu = g\beta H_0$. The lineshape parameters obtained by fitting, i.e. the g factor, the peak to peak linewidth ΔH_{pp} and the product of the intensity with temperature $I \times T$ are plotted in figure 2 along with the data of PCMO-h obtained earlier by us [12]. The intensities were obtained as the best fit values to the parameter 'A' in equation (2). This eliminates some of the problems encountered in obtaining it from double integration of the derivatives if the baseline is not correctly determined. We would like to emphasize here that the fits of the signals to the respective equations were excellent and the fitting errors were much smaller than the sizes of the data points. The error bars on the 'g' values plotted in figure 2(a) indicate the precision of the measurement of H_0 (± 3 G) converted to the error in 'g' (± 0.002). Actual fitting errors were much less than this value.

Now we compare the EPR parameters obtained from the two manganites. The linewidth (figure 1(a)) behaves differently in the two manganites as a function of temperature. In PCMO-e it shows a slight monotonic decrease down to 245 K below which it shows a smooth, sharper increase. In PCMO-h on the other hand, there is a sharp discontinuous increase at T_{co} and a monotonic but much slower increase at lower temperatures.

The asymmetry parameter α plotted in figure 1(b) exhibits marked differences between the two samples. In PCMO-h, it goes through an anomalous peak at T_{co} before showing the

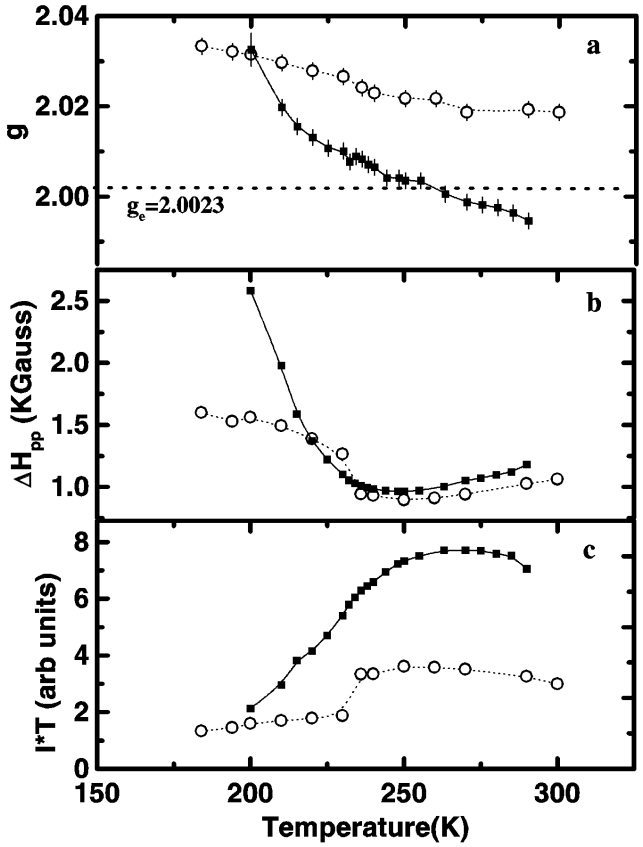

Figure 2. Temperature dependence of powder lineshape parameters: (a) g (the vertical lines show error bars on the 'g' value), (b) the peak to peak linewidths ΔH_{pp} and (c) intensity times T. The error bars for the ΔH_{pp} and intensity are very small and hence are not shown. The open circles represent the data for PCMO-h and the solid squares for PCMO-e. The curves (dotted and solid, respectively) are guides to the eye. The data for PCMO-h are reproduced for the sake of comparison from [12].

expected decrease (due to the increase in the skin depth consequent to the increase in resistivity below T_{co}), while in PCMO-e, this peak is conspicuously absent.

We note here that in manganites the single crystal 'g' value might have a contribution from the local fields as discussed in [12] and [13]. In powder samples the individual grains are randomly orientated. The local fields due to these grains can affect the lineshape and width, but since their net effect is symmetric around the centre field, the latter remains unaltered. Another way of looking at it is in terms of a mutual cancellation of oppositely oriented local fields resulting in no change in the centre field, leaving the 'g' value unaffected. Therefore, we focus on the powder data for the comparison of 'g' values.

In figure 2, we show the results from the powder spectra of PCMO-h and PCMO-e. Experimentally the EPR spectra from $Pr_{1-x}Ca_xMnO_3$, like those from most manganites in their paramagnetic phase, are simple: a single, relatively broad, symmetric Lorentzian (in the case of powdered samples) or an asymmetric Dysonian (in the single crystal samples) is observed. However, understanding the origin of these signals is far from straightforward, as discussed in our earlier work [13]. We note that there are at least two different kinds of

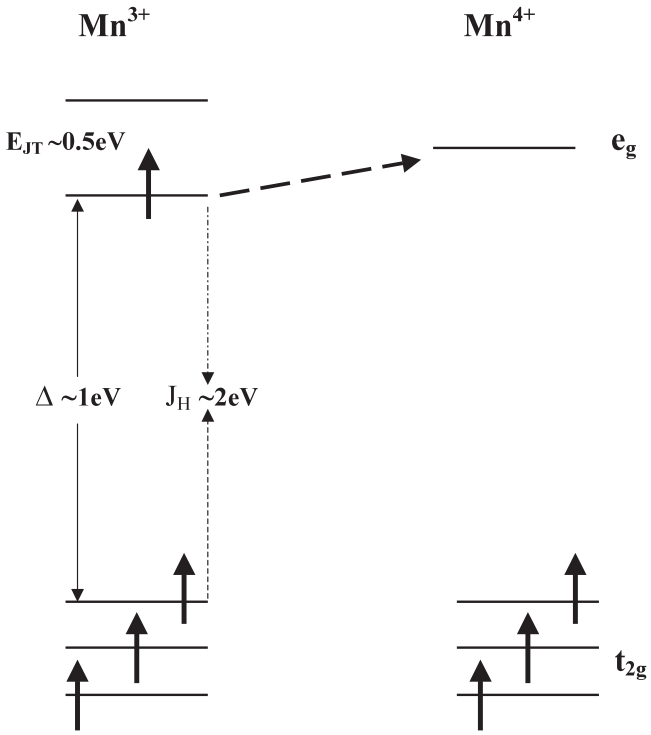

Figure 3. Schematic diagram of electronic energy levels of manganites, such as PCMO-e, relevant to EPR. The five-fold degeneracy of the 3d orbitals are split into a t_{2g} triplet and an e_g doublet which is further split by the Jahn–Teller effect. Typical energy scales of different interactions are also indicated. The t_{2g} and the e_g spins are very strongly Hund-coupled [1].

paramagnetic centres, namely, Mn^{3+} (d^4, $S = 2$) and Mn^{4+} (d^3, $S = 3/2$). These form an extended lattice and are therefore subjected to strong exchange and dipolar interactions. It is an accepted practice in EPR literature to treat this essentially band problem in terms of a Zeeman Hamiltonian which is a sum of the Zeeman Hamiltonians of the individual spins to which the exchange and the dipolar interactions are added perturbatively [14]. An added feature of the EPR in manganites is that the fourth electron (or 'hole') of Mn^{3+} placed in the Jahn–Teller split e_g orbital, though strongly Hund-coupled to the core t_{2g} spins (figure 3), is not stationary. It is hopping between the Mn^{3+} and Mn^{4+} sites (via the intervening oxygen) either by the Zener double exchange mechanism (in the case of the CMR manganites) or as a Jahn–Teller polaron (in the case of the CO manganites). It has been shown earlier that all the Mn ions contribute to the EPR signal, which is strongly exchange narrowed leading to a single featureless signal. Thus we understand the EPR signal to originate from the strongly coupled Mn^{3+} and Mn^{4+} ions with the (partially) itinerant nature of the e_g electron (or 'hole') having significant influence on the nature of the spectra depending on the rate of its hopping.

Very strikingly the g value at room temperature in PCMO-e is less than the free electron g value 'g_e', while PCMO-h exhibits an anomalous (see below), positive g shift. The 'g' values plotted in figure 2(a) show a monotonic increase as the temperature is reduced from room temperature in both the compounds. The magnitude of 'g' in the former is however greater than 'g_e' throughout the temperature range whereas in the latter it shows a crossover from less than 'g_e' to a value larger than 'g_e' near T_{co}. Also, the temperature dependence of 'g' in the

two samples is qualitatively different. The variation of 'g' from room temperature down to T_N is much larger in PCMO-e than in PCMO-h.

The dependence of the peak to peak linewidth ΔH_{pp} on temperature shown in figure 2(b) for PCMO-h and PCMO-e also shows a difference below T_{co} in that the curvatures of the two are opposite to each other. The variation in linewidth is again larger in PCMO-e than in PCMO-h.

The EPR intensities for the two samples are plotted in figures 2(c) against temperature. In both the samples, the intensity goes through a peak at T_{co}, decreasing monotonically below this temperature. However, the sharp drop in intensity found at $\sim T_{co}$ (240 K) in the case of PCMO-h is not seen in PCMO-e.

Now we attempt to understand these results in the light of the microscopic phenomena occurring in these systems. We focus on the magnitude and the temperature variation of 'g' in the powder sample and that of ΔH and α in single crystals. The departure of g value from 'g_e' is given by $g = g_e(1 - k\frac{\lambda}{\Delta})$ where λ is the spin–orbit coupling constant, k is a positive numerical factor and Δ is the crystal field splitting [16]. In PCMO-h even in the charge disordered paramagnetic state, the g value was larger than 'g_e' and on cooling stayed independent of temperature until T_{co}. Below T_{co} it became very sensitive to temperature and went on increasing with decreasing temperature. The anomalous 'g' shift (since for both Mn^{3+} and Mn^{4+} 'g' is expected to be lower than 'g_e') could be attributed to the 'hole' nature of the charge carriers since for holes in a less than half filled shell the spin–orbit coupling constant λ is negative [17]. Our present study on PCMO-e provides additional support to this explanation since with electrons as charge carriers, 'g' is less than 'g_e', as expected, in the charge disordered state. The increase in 'g' below T_{co} found in PCMO-h and $Nd_{0.5}Ca_{0.5}MnO_3$ (NCMO) [13] was attributed to the strengthening of the spin–orbit interaction and spin-other orbit interaction due to orbital ordering developing between T_{co} and T_N. However, the fact that 'g' crosses over to a value greater than 'g_e' in the electron-doped system and continues to increase as the temperature is lowered below T_{co} indicates that an essentially different mechanism is operative in the electron-doped system. This is consistent with the suggestion by Khomskii [18] that in these systems the concept of orbital ordering cannot be strictly applied.

Now we analyse the temperature dependence of linewidth in single crystals of PCMO-e and PCMO-h. We wish to point out that the effect of local fields on the g value and the linewidth will be different. The g value is determined by the centre field which would be affected if there is a net local field adding to or subtracting from the applied field. Such a situation is easily obtainable in the case of a single crystal where there can be non-random orientations of local fields in different smaller regions, whereas in a powder random orientations of such local fields will make the net effect on the measured g value zero. However, the same random orientations of the local fields will add to the linewidths in powders (due to inhomogeneous broadening) though in single crystals this effect will be minimal.

It is also more appropriate to use single crystal data for the linewidth behaviour because of the following reasons: with decrease in particle size, surface effects begin to dominate over the intrinsic effects. For example, in the case of CESR, linewidths have been found to be dependent upon the size of the sample (thickness of the sample in the micrometre range). Moreover, rates of diffusion in confined geometries are found to be different for those in the bulk. To be sure, the linewidths of our single crystal samples are larger than those of the micrometre sized powdered particles dispersed in paraffin wax. (This is NOT the same as the size dependent linewidth observed in magnetically ordered manganites where it happens because of excessive loading of the cavity [6]. In our experiments the loading of the cavity as observed by any visible change in the detector current was minimal.) While the actual details of the effect of the size of the particles on the linewidth in the charge ordered manganites

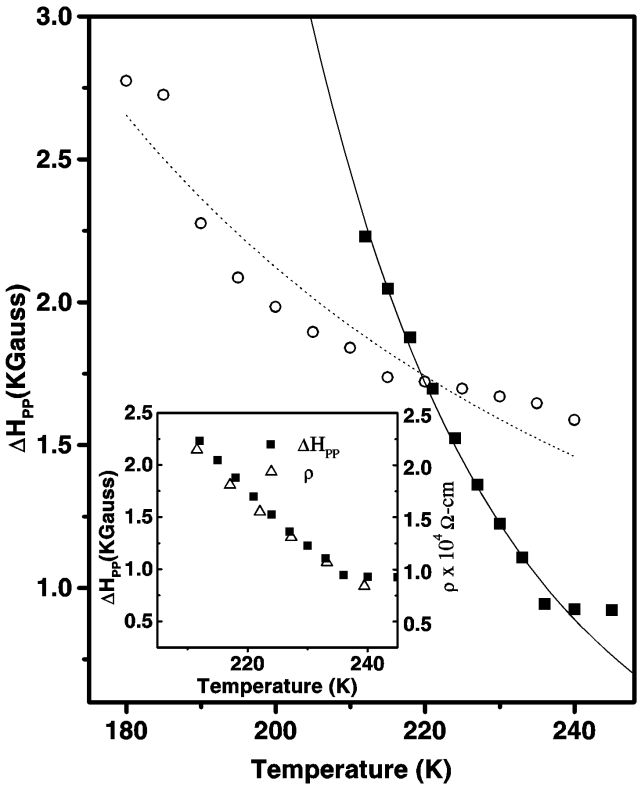

Figure 4. Temperature dependence of single crystal linewidths $\Delta H_{\rm pp}$. The solid squares are the data for PCMO-e and the open circles for PCMO-h. The solid and the dotted curves are the least square fits to the variable range hopping model (equation (3)) to the respective data sets in the temperature range $T_{\rm N}$ to $T_{\rm co}$. The inset shows the essentially similar temperature dependence of the resistivity (open triangles, obtained from [3], scaled by an appropriate constant), and $\Delta H_{\rm pp}$ (solid triangles) data for PCMO-e.

are yet to be worked out at this stage, we want to make the point that the linewidth of single crystals of a few millimetres thickness are expected to reflect the intrinsic behaviour more than the micrometre sized particles in powder. Therefore we analyse the single crystal data to understand the temperature dependence of the linewidth.

It has been observed that in the hole-doped PCMO and NCMO the dependence of ΔH on T in the single crystals in the region $T_{\rm N} \leqslant T \leqslant T_{\rm co}$ could be explained in terms of a model involving motional narrowing [13]. Hopping of the Jahn–Teller polarons was understood to be the underlying mechanism of charge transport. However, we notice in figures 1(a) and 4 that ΔH versus T of PCMO-e and PCMO-h have different functional dependences on temperature. Interestingly we observe that in PCMO-e the temperature dependence of the resistivity ρ is the same as the temperature dependence of $\Delta H_{\rm pp}$ of single crystals, as shown in the inset of figure 4. We find that both the resistivity and the single crystal EPR linewidth fit the model of variable range hopping (VRH) (solid curve in figure 4) given by the equation

$$\Delta H = K \exp\left(\frac{T_0}{T}\right)^{\frac{1}{4}}. \tag{3}$$

VRH has been earlier used to explain the resistivity of manganites in the paramagnetic state by a number of different workers [19–21]. Viret *et al* [21], using the concept of magnetic localization, found that the density of states gets modified consequent to the localization of charge carriers due to Hund's coupling between the itinerant e_g electrons and the stationary, core t_{2g} spins. This leads to the realization of a random potential in the paramagnetic state. In the case of CO manganites, in the charge ordered state a long ranged AFM order is not established. So the concept of random magnetic potential can be applied. From the VRH fit we obtained the parameter T_0. The localization length is given by $\frac{1}{\beta} = \sqrt[3]{\frac{kT_0}{171U_m v}}$ where k is the Boltzmann factor, U_m is the random magnetic potential which is of the order of 2 eV (Hund's coupling) and v is the volume of the unit cell per manganese ion which is 5.7×10^{-29} m^3. The numerical factor 171 comes following Viret *et al* [21] from the geometrical corrections due to the symmetry of the d_{z^2} orbital of the e_g electron and the probability that an unoccupied manganese orbital can accept an electron. The localization length for PCMO-e thus obtained is 0.3 nm which is larger than the Mn ionic radius ($\sim$0.72 Å for Mn^{3+} and $\sim$0.65 Å for Mn^{4+}), of the same order as the Mn–Mn distance and smaller than the hopping distance of 1.5 nm, as expected in the VRH model [21]. While the VRH fit to ΔH_{pp} versus T in PCMO-e is seen to be excellent, the model did not fit the linewidth data of PCMO-h well (dotted curve in figure 4), the regression coefficient indicative of the goodness of fit being 0.91 in the latter compared to 0.99 for the fit to the data of PCMO-e.

The same conclusion, i.e. the non-applicability of the model of motional narrowing in the case of PCMO-e, is borne out by the behaviour of α as well. In the case of PCMO-h, an anomalous peak is observed in α versus T at T_{co}. No such peak is observed in PCMO-e where α decreases smoothly as ρ increases below T_{co}, as expected. In PCMO-h, the peak in α was found to be correlated with the motion of the Jahn–Teller polarons. The absence of such a peak in PCMO-e again points towards the negligible contribution of Jahn–Teller polaron-mediated charge transport in this system.

In summary, the comparative EPR study of hole-doped and electron-doped PCMO brings out certain essential differences in the nature of the order and the transport mechanisms in the two cases.

Acknowledgments

AKS and SVB thank Department of Science and Technology and the University Grant Commission for financial support. JJ thanks CSIR, India for a fellowship. CNRR thanks the BRNS (DAE) for support.

References

[1] Rao C N R and Raveau B (ed) 1998 *Colossal Magnetoresistance, Charge Ordering and Related Properties of Manganese Oxides* (Singapore: World Scientific)
[2] Tokura Y 2000 *Colossal Magnetoresistive Oxides* (New York: Gordon and Breach)
[3] Vijaya Sarathy K, Vanitha P V, Seshadri R, Cheetham A K and Rao C N R 2001 *Chem. Mater.* **13** 787
[4] Oseroff S B, Torikachvili M, Singley J, Ali S, Cheong S-W and Schultz S 1996 *Phys. Rev.* B **53** 6521
[5] Rivadulla F, Lopez-Quintela M A, Hueso L E, Rivas J, Causa M T, Ramos C, Sanchez R D and Tovar M 1999 *Phys. Rev.* **60** 11922
[6] Causa M T, Tovar M, Caneiro A, Prado F, Ibanez G, Ramos C A, Butera A, Alascio B, Obrados X, Pinol S, Rivadulla F, Vazquez-Vazquez C, Lopez-Quintela M A, Rivas J, Tokura Y and Oseroff S B 1998 *Phys. Rev.* B **58** 3233
[7] Tovar M, Alejandro G, Butera A, Caneiro A, Causa M T, Prado F and Sanchez R D 1999 *Phys. Rev.* B **60** 10199
[8] Shengelaya A, Zhao G M, Keller H and Muller K A 1996 *Phys. Rev. Lett.* **77** 5296

[9] Lofland S E, Kim P, Dahiroc P, Bhagat S M, Tyagi S D, Karabashev S G, Shulyatev D A, Arsenov A A and Mukovskii Y 1997 *Phys. Lett.* A **233** 476
[10] Ivanshin V A, Deisenhofer J, Krug von Nidda H-A, Loidl A, Mukhin A A, Balbashov A M and Eremin M V 2000 *Phys. Rev.* B **61** 6213
[11] Shengelaya A, Zhao G-M, Keller H, Muller K A and Kochelaev B I 2000 *Phys. Rev.* B **61** 5888
[12] Gupta R, Joshi J P, Bhat S V, Sood A K and Rao C N R 2000 *J. Phys.: Condens. Matter* **12** 6919
[13] Joshi J P, Gupta R, Sood A K, Bhat S V, Raju A R and Rao C N R 2002 *Phys. Rev.* B **65** 024410
[14] Bencini A and Gatteschi D 1989 *Electron Paramagnetic Resonance of Exchange Coupled Systems* (Berlin: Springer) p 135
[15] Dupont F, Millange F, DeBrion S, Janossy A and Chouteau G 2001 *Phys. Rev.* B **64** 220403
[16] Abragam A and Bleaney B 1970 *Electron Paramagnetic Resonance of Transition Ions* (Oxford: Clarendon)
[17] Weltner W Jr 1983 *Magnetic Atoms and Molecules* (New York: Van Nostrand-Reinhold) p 47
[18] Khomskii D I 2001 *Int. J. Mod. Phys.* B **15** 2665
[19] Satyalakshmi K M, Fisher B, Patlagan L, Koren G, Sheriff E, Prozorov R and Yeshurun Y 1998 *Appl. Phys. Lett.* **73** 402
[20] Anil Kumar P S, Joy P A and Date S K 1998 *J. Phys.: Condens. Matter* **10** L269
[21] Viret M, Ranno L and Coey J M D 1997 *Phys. Rev.* B **55** 8067